Arch. Metall. Mater., Vol. 61 (2016), No 2, p. 731–740

DOI: 10.1515/amm-2016-0125

S. STANO*, A. GRAJCAR**,#, Z. WILK**, M. RÓŻAŃSKI*, P. MATTER**, M. MORAWIEC**

MICROSTRUCTURAL ASPECTS OF TWIN-SPOT LASER WELDING OF DP-HSLA STEEL SHEET JOINTS

The article presents the possibility of using twin-spot laser welding (i.e. laser welding with focusing a laser beam on two spots) for making overlap joints made of 0.8-1 mm thick HSLA and DP type high strength steel sheets. Joints were made using a Yb:YAG disc laser having a maximum power of 12 kW and a welding head by means of which it was possible to focus a laser beam on two spots, 0.6 mm and 1 mm away. The angle between focuses amounted to 0° or 90°, whereas the power distribution was 50%-50%. With settings as presented above it was possible to obtain high-quality overlap joints. The geometrical parameters of the joints were primarily affected by beams positions (in relation to each other) and, to a lesser degree, by the distance between the focuses. It was possible to obtain a 10% hardness reduction in the fusion zone of the DP-HSLA steel joints if the angle between the beams amounted to 90°. The tests also involved microstructural examinations of individual zones of the joints.

Keywords: DP steel, HSLA steel, weldability, overlap joint, twin-spot welding

1. Introduction

Due to its numerous advantages, resistance welding is the most common when joining car bodies [1]. Increasingly frequently, high efficiency can also be achieved by means of laser welding. New solid state lasers and their application as generators of laser radiation for welding in the automotive industry were summarised by Stano [2]. Laser welding is frequently used when joining thermomechanically rolled HSLA (High Strength Low Alloy) steels [3-5]. The application of different types of lasers for welding was reviewed by Lisiecki [6]. Recently, increasingly common in the automotive industry are AHSS (Advanced High Strength Steels), as described by Grajcar et al. [7] and Lasek and Mazancova [8]. Their excellent combination of strength and plasticity results from the proper distribution of hard and soft structural components, leading to high strain hardening rates during plastic deformation [9]. The most commonly applied steels from this group include Dual Phase (DP) steels [10] and TRansformation Induced Plasticity (TRIP) multiphase steels [11, 12]. So far, laser welding of HSLA-DP type joints has not been the subject of sufficient attention.

In most cases, laser welding is performed by focusing a laser beam on one spot [13]. The appropriate power density in the area affected by a laser beam enables to obtain a gasodynamic channel, i.e. a deep and narrow capillary filled with gases and metallic vapours [14]. Welds obtained in such a manner are characterised by a narrow face in comparison with a penetration depth. In addition, such a manner of laser welding enables to obtain high welding rates, narrow heat affected zone (HAZ) and minimum welding strains. However, it also requires high accuracy when matching elements to be welded and when positioning these elements in the operational space of a manipulator positioning the working head [15]. It should also be noted that the high welding rates (very low linear energy) can trigger disadvantageous phenomena during the crystallisation of a weld, e.g. cracks or excessive hardness in a weld or in the HAZ [16].

The microstructure and mechanical properties of a laser welded joint are affected by numerous laser welding parameters. Kong et al. [17] modelled the temperature field and grain growth of DP980 steel under conditions of a laser heat treatment. They demonstrated that the increased scanning rate of the laser beam under laser power of 2 kW decreased the temperature gradient in the HAZ resulting in finer martensite laths. As regards high strength DP steels, a frequent problem is the formation of a soft zone connected with the tempering of martensite [18]. Such a soft zone in the outer HAZ due to the tempering of pre-existing martensite in the DP600 steel was identified by Farabi et al. [19]. Li et al. [20] reported that the width of the soft zone in the DP1000 sheet steel and its distance from the weld centre increased along with increasing values of laser power and decreasing welding rates.

The reduction of hardness in the fusion zone and in the HAZ can be obtained by using various pre- and post-heat treatments related to the modification of thermal cycles [21]. It is expected that one of the manners allowing the reduction of inconvenient microstructural phenomena taking place during laser welding can be the use of a laser welding technique where a beam is focused on two spots, also referred to as “twin-spot”, “bi-focal” or “dual beam” welding [22]. This study aims to determine the effect of various twin-spot laser welding parameters on the microstructure of HSLA-DP steel joints.

* INSTITUTE OF WELDING, 16-18 BL. CZESŁAWA STR., 44-100 GLIWICE, POLAND

** SILESIAN UNIVERSITY OF TECHNOLOGY, 18A KONARSKIEGO STR., 44-100 GLIWICE, POLAND

Corresponding author: adam.grajcar@polsl.pl

2. Experimental procedure

2.1. Material

The study-related tests involved making overlap joints using 1 mm thick DOCOL 800DP and 0.8 mm thick HC420LA grade steel sheets. The specimens made of the HSLA steel sheet were placed on the DP (dual phase) type steel sheet. As regards its geometry, such a type of joint corresponds to the joints frequently used in industrial conditions. Directly before laser welding the sheets were subjected to degreasing using acetone. Table 1 presents the chemical composition and mechanical properties of the steel sheets according to the manufacturer (SSAB). The HSLA steel (commercial name: Docol H420LA) is used for making sheets which should be characterised by higher strength and good formability when subjected to cold processing. The steel minimum bend radius for 90° amounts to 0.25 of the sheet thickness. The DP800 steel is characterised by the advantageous combination of formability and strength. The steel minimum bend radius for 90° amounts to 1.00 of the sheet thickness [23].

2.2. Dual beam laser welding tests

The test overlap joints were made using a TruDisk 12002 disc laser having a maximum power of 12 kW and a Trumph D70 welding head, by means of which a laser beam was focused on two spots. The head and the resonator were connected using a system of optical fibres with diameters of 200µm, 300µm, 400µm and 600µm. The welding process was automated and performed on a station equipped with a KUKA KR30HA industrial robot. The power distribution density of both beams was checked using a Prometec UFF100 laser beam analyser. The appropriately selected optical fibre and lens enabled the obtainment of a beam having a diameter of 0.6 mm. Further details concerned with the welding station and its technological tooling can be found elsewhere [24].

The power density of the laser beam focused on two spots was changed by inserting an optical filter across the laser beam trajectory and adjusting its position using an adjustment screw. The head enabled the adjustment of 30%-70% laser beam power distribution. The power distribution adopted in the tests was 50%-50%. In addition, the D70 head was provided with a system positioning the beam focus in relation to the direction of welding.

Reference experiments were laser beam tests utilising a single beam and leading to the obtainment of entire penetration with a scanning rate of 11 and 12 m/min. Laser welding focused on two spots was performed for distances between focuses amounting to 0.6 and 1 mm, and for beams positioned at angles of 0° and 90° in relation to the direction of welding (Table 2). The value of laser beam power adopted for both single and double spot focusing was the same (P = 6 kW). The beam focus position was f = 0 mm (focusing on the surface of elements being welded). The welding rate range adopted in the major experiments was 8.5-10 m/min. In the tests with beams positioned perpendicularly, a welding rate was changed experimentally and restricted within the range of 5 to 9 m/min. Such an approach was adopted in order to obtain various degrees of penetration on the sheet pack thickness. Table 2 presents detailed parameters of the basic laser welding tests with the beam focused on one and two spots. Fig. 1 presents the positions of the twin-spot system focuses in relation to the direction of welding as well as exemplary power density distributions of the laser beam for the focus position on the surface of elements being welded (f = 0 mm).

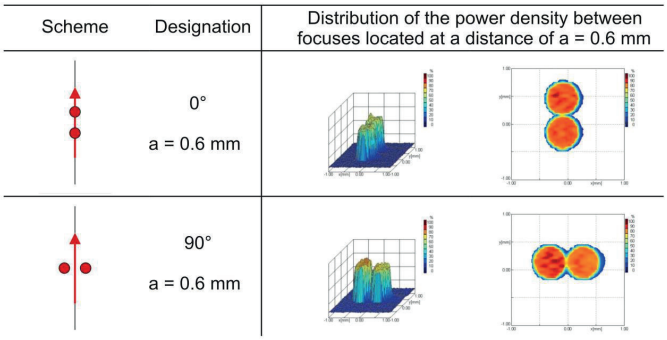

Fig. 1. Position of focuses in the twin-spot system in relation to the direction of welding and exemplary distributions of laser beam power density for focuses positioned on the surfaces of elements being welded (f = 0 mm)

TABLE 1

Chemical composition (in wt.%) and mechanical properties of the tested steels provided by the manufacturer

Steel grade	YS (MPa)	UTS (MPa)	TEl (%)	C	Si	Mn	P	S	Al	Nb	Ti
800DP	500-650	800-950	10	0.14	0.20	1.50	0.010	0.002	0.040	0.015	-
HC420LA	420-520	470-590	17	0.10	0.50	1.60	0.025	0.025	0.015	0.090	0.150

TABLE 2

Single and dual beam laser welding parameters

No.	Spot number	Scanning rate (m/min)	Distance between spots (mm)	Beam power (W)	Beam power distribution (%)	Angle between spots (°)	Heat input (kJ/mm)
1	1 spot	11 or 12	-	6000	-	-	0.033 or 0.03
2	2 spots	8.5-10	0.6	6000	50:50	0	0.040
3	2 spots	8.5-10	1.0	6000	50:50	0	0.040
4	2 spots	5-9	0.6	6000	50:50	90	0.040
5	2 spots	5-9	1.0	6000	50:50	90	0.040

2.3. Macro- and microstructure investigations

The first step of investigations involved visual inspection and macroscopic examinations. The assessment related to the effect of the position of two focuses of the laser beam in relation to the welding direction on a welding rate (geometric parameters of welds) was based on the data gathered when investigating the specimens with the entire penetration (as the objective criterion of joint evaluation). As regards the welding tests without achieving the entire penetration, the adopted welding rates did not guarantee the obtainment of the same penetration depth in each case and the objective assessment of the geometric parameters of the weld. Before macro- and microscopic observations the metallographic specimens were subjected to grinding with abrasive papers (granularity of 200, 400, 600, 1000 and 1200) followed by polishing. Afterwards, the specimens were etched in nital for 4 seconds and subjected to microscopic observations (magnification between 25x and 1000x). Some details of the microstructure were revealed using SEM.

2.4. Hardness measurements

Hardness measurements utilising the Vickers test (HV5) involved the specimens without the entire penetration. As these specimens were made at higher welding rates, it was expected that their hardness test result values would be higher than those of the joints made at lower welding rates. The measurements were conducted in two measurement lines corresponding to the geometrical centres of the HSLA and DP steel sheets joined. Due to a very small area affected by the heat, three hardness measurements in the HAZ were performed (points: 4-6 and 10-12).

3. Results and discussion

3.1. Macrostructure of single spot laser welding specimens

The tests of laser welding with the beam focused on one spot (treated as reference tests) revealed that for a laser beam power of 6 kW, the entire penetration of sheets being joined was obtained at a welding rate of 11 m/min. The weld obtained was very narrow, with almost parallel fusion lines becoming narrow in the weld root area (Fig. 2a). At the interface of the two sheets the weld width amounted to approximately 0.9 mm. The very high dynamics of the process resulted in small spatter visible in weld face area. However, the aforesaid spatter did not significantly reduce the weld face. When a welding rate was increased to 12 m/min, the entire penetration was not obtained (Fig. 2b); only the penetration into the lower sheet (0.78 mm deep) was achieved, with the same weld width maintained at the interface of the sheets. Various widths of the HAZ for different steel grade sheets demonstrated various material properties of the sheets being joined and revealed greater crack susceptibility in the joint area. Hardness measurements revealed a significant hardness increase in the weld and in the HAZ. Outside these areas, the HSLA steel was characterised by lower hardness than that of the DP steel, which was consistent with the test results concerning mechanical properties (see Table 1).

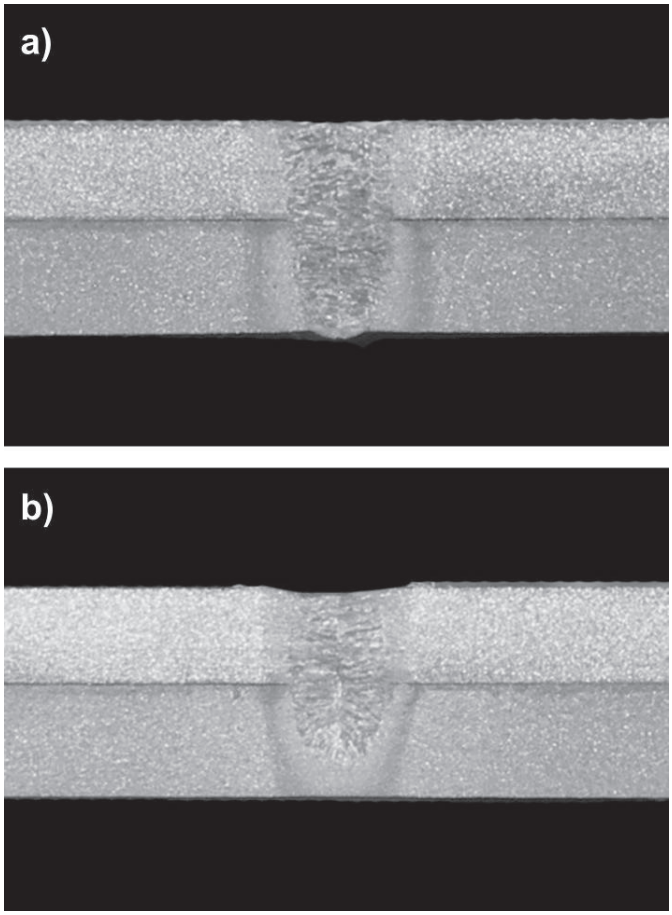

Fig. 2. Macrostructure and the face of the weld in the overlap joint made using a laser beam focused on one spot: welding rate: 11 m/min (a) and 12 m/min (b)

3.2. Macrostructure of twin-spot laser welding specimens

In comparison with laser welding utilising a single beam, the use of the twin-spot technique (with beams positioned at 90° in relation to the direction of welding) required the reduction of a welding rate in order to obtain the entire penetration. The weld made in such a manner was wide, with fusion lines slightly converging at the bottom (Fig. 3). Increasing the inter-beam distance from 0.6 mm to 1 mm and arranging them in series (i.e. at 0° in relation to the direction of welding) made it possible to increase a welding rate by 70% without compromising the obtainment of entire penetration (Fig. 4). However, such an approach resulted in the narrowing of the joint of the sheets by almost 40%. In spite of the changed conditions, the weld face remained wide, being by 18% narrower than in the previous test.

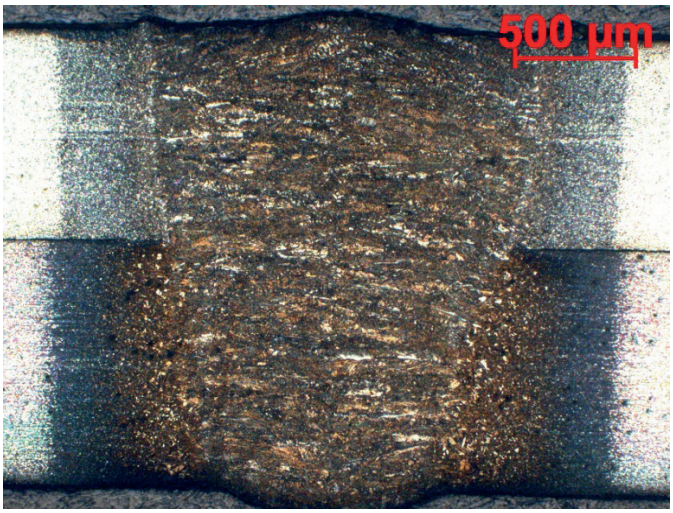

Fig. 3. Macrostructure of the joint welded using a dual beam positioned perpendicularly in relation to the direction of welding, welding rate: 5 m/s, distance between the beams: 0.6 mm

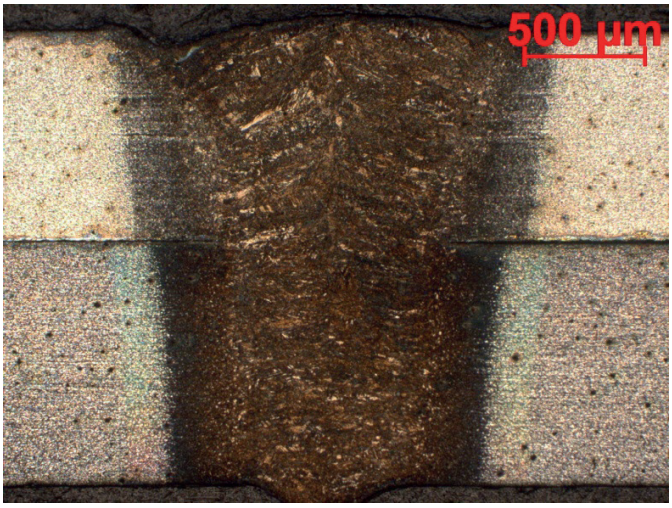

Fig. 4. Macrostructure of the joint welded using a dual beam positioned in series; welding rate: 9 m/min, distance between the beams: 1 mm

Positioning the beams at an angle of 90° in relation to the direction of welding repeatedly led to the formation of the wide joint of sheets (Fig. 5a) in comparison with the joints made with beams positioned at an angle of 0° (Fig. 5b and c). Fig. 6 presents the comparison of the maximum welding rates ensuring the obtainment of the entire penetration for various positions of focuses and distances between them. The use of a laser beam focused on two spots decreased the maximum welding rate. The focuses positioned at an angle of 90° decreased the welding rate to 5 m/min. When the focuses were at an angle of 0°, a decrease in the welding rate (compared with single beam laser welding) was slight, i.e. approximately 1.5 m/min. Increasing the distance between the focuses from 0.6 mm to 1 mm had an insignificant effect on the reduction of the maximum welding rate.

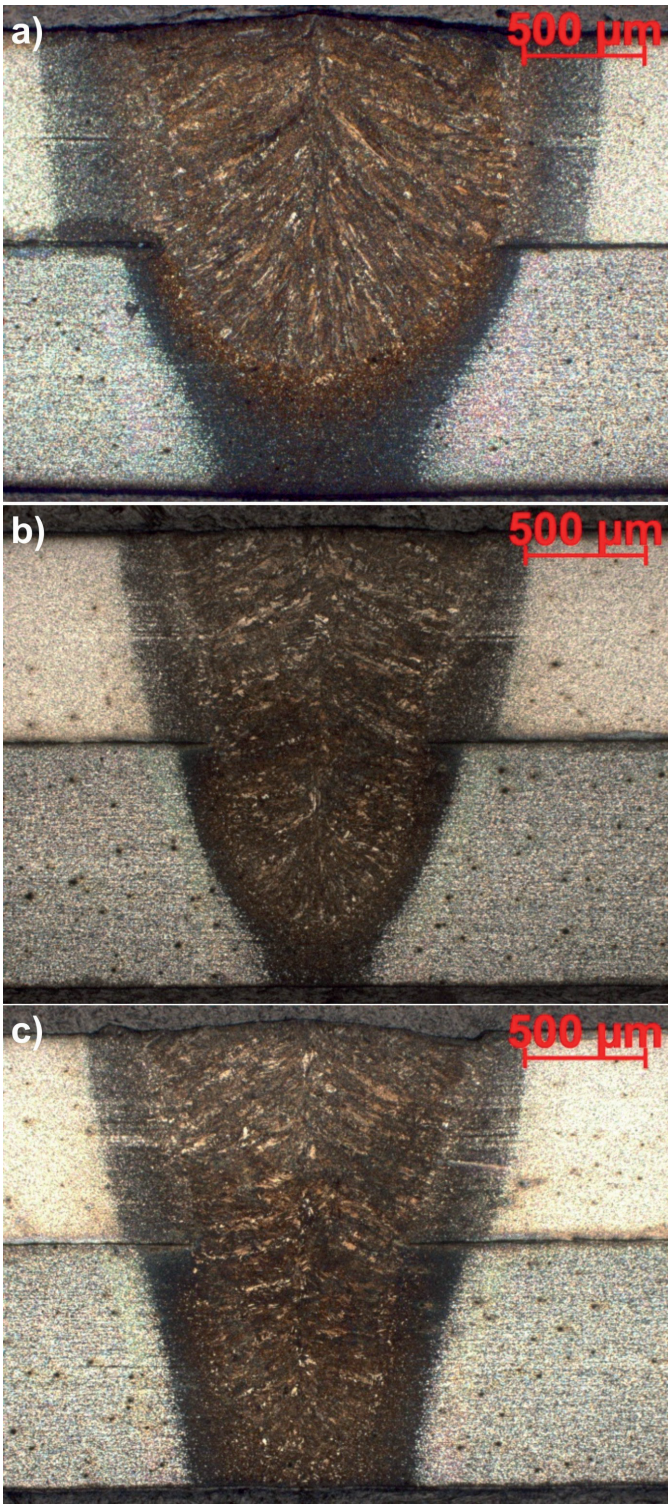

Fig. 5. Macrostructure of the joint welded using a laser beam: a) V = 6m/min, angle 90°, distance between the beams 0.6 mm; b) V = 10m/min, angle 0°, distance between the beams 1 mm; c) V = 9.5m/min, angle 0°, distance between the beams 0.6 mm

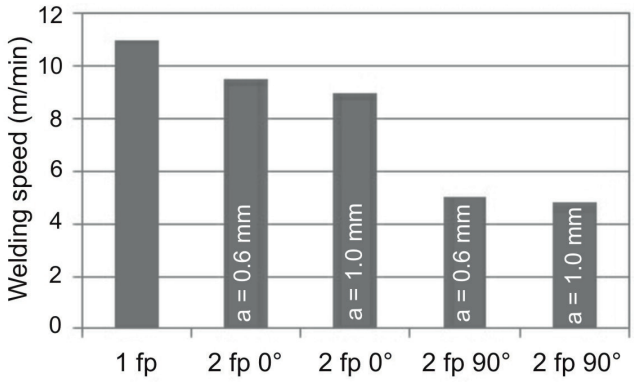

Fig. 6. Maximum welding rates allowing the obtainment of the entire penetration for various positions of laser beam focuses and distances between them; distance between the beams 0.6 mm

Both welding with a single beam and welding with a beam focused on two spots at an angle of 0° leads to the formation of a V-shaped weld (Fig. 1 and 5b). The width of the fusion area at the interface of sheets, determining the cross-section of the weld and the strength of a welded joint, amounts to approximately 0.8 mm for 0° (Fig. 7). The wider area affected by the laser beam in the plane perpendicular to the direction of welding (at an angle of 90°) increased the geometrical dimensions of the weld. For the beam positioned at an angle of 90°, the width of a joint was two times greater. The transverse position of focuses in relation to the scanning direction caused the formation of a weld having very similar widths of the face, joint and root (Fig. 7). Increasing the distance between the laser beam focuses from 0.6 mm do 1 mm increased the widths of the face, root and joint.

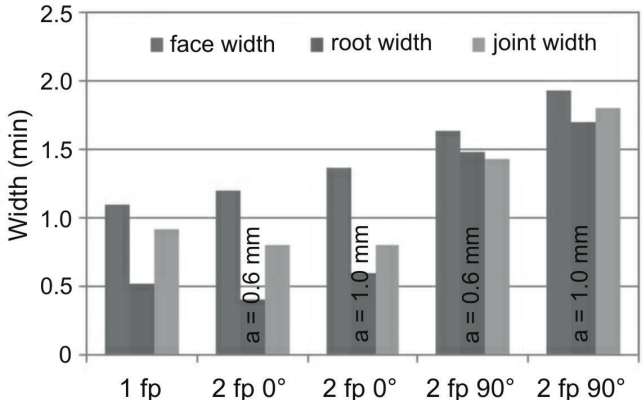

Fig. 7. Characteristic dimensions of welds with the entire penetration for various positions of laser beam focuses and distances between them; distance between the beams 0.6 mm

3.3. Effect of welding rate on macrostructure

The welding rate is the key parameter of the welding process as it is directly connected with the linear energy. The welding rate is mainly responsible for the shape and dimensions of joints, is decisive for the hardness of a joint and, from the technological point of view, is connected with process efficiency. Fig. 8 presents the macrostructures of specimens made in the same conditions except for scanning rates. The greater the amount of energy absorbed by the material, the wider the joint zones in both sheets, with their ratio close to unity. The same result was obtained at a welding rate of 8.5 m/min, where fusion lines were almost parallel, particularly in the bottom sheet (Fig. 8a). An increase in a beam scanning rate from 8.5 m/min to 10 m/min was accompanied by a decrease in the linear energy from 0.042 kJ/mm to 0.036 kJ/mm, by the change of the weld shape (increasingly similar to the letter V) and by a shallower penetration depth. At the maximum scanning rate it was impossible to obtain the entire penetration (Fig. 8d).

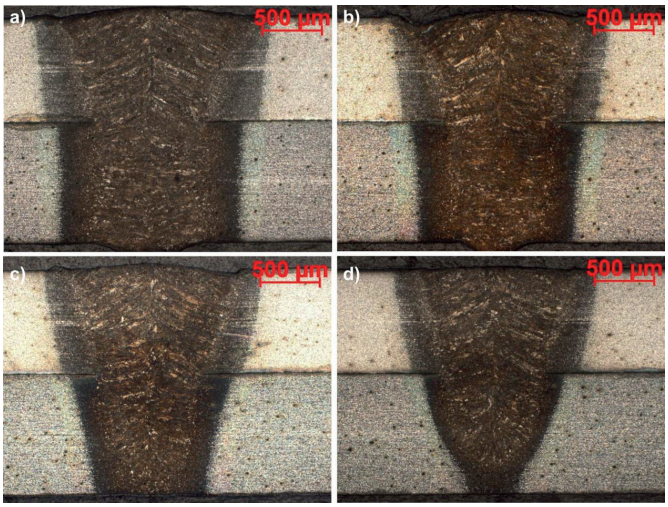

Fig. 8. Macrostructure of the joints welded with the following welding rates: a) 8.5 m/min, b) 9 m/min, c) 9.5 m/min, d) 10 m/min; angle between the beams and the direction of welding: 0°; distance between the beams: 1 mm

3.4. Microstructure of base materials

Both steels were characterised by significant refinement, hence the identification of their structural components required a magnification of at least 1000x. Fig. 9 presents the microstructure of the base material of the DP800 steel. The microstructure was composed of ferrite grains with sizes in the range of 4 to10 µm, surrounded by the layer of martensite on each side. The martensite content amounted to approximately 45%. It was calculated as the difference between 100% and a ferrite content determined by the image analysis. Islands of martensite were not separated in the ferritic matrix, but formed a continuous envelope. It was also possible to notice certain structural banding resulting from the rolling of sheets.

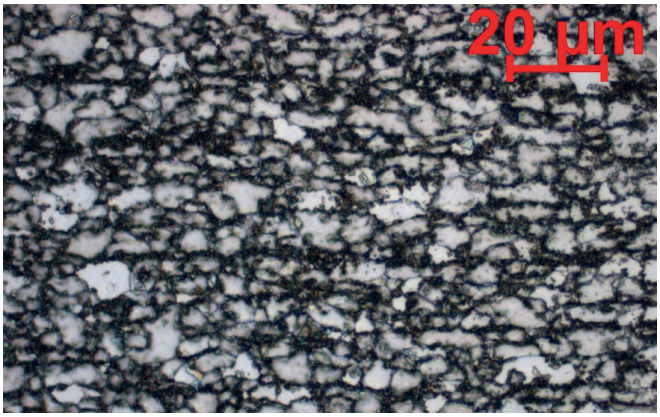

Fig. 9. Microstructure of DP800 steel magnified 1000x

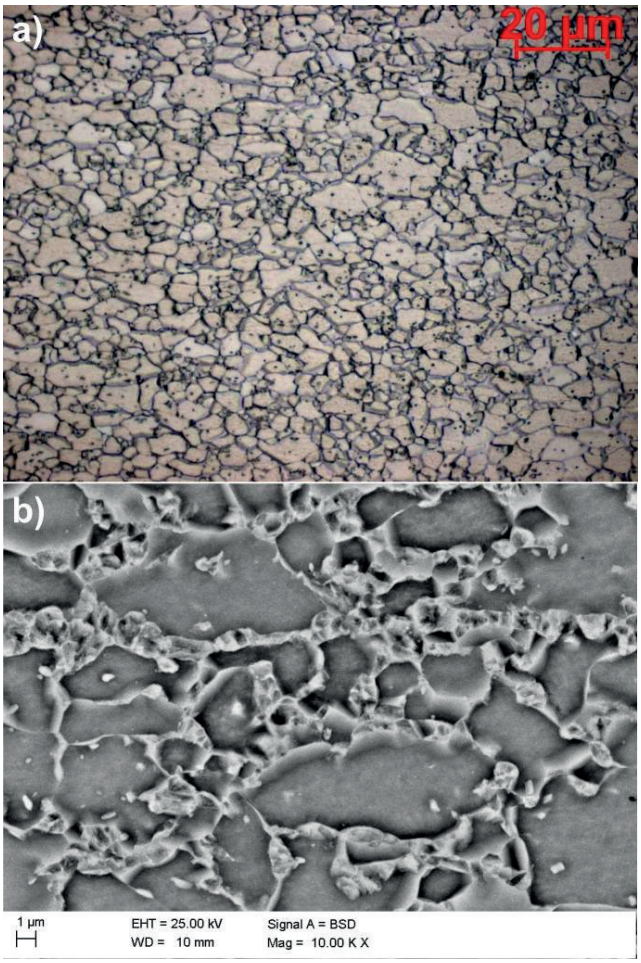

Fig. 10. LOM (a) and SEM (b) micrographs of HC420LA steel

The microstructure of the HC420LA was composed of ferritic matrix and pearlitic islands (Fig. 10a). The content of the pearlite was lower than the volume fraction of martensite in the DP steel. Additionally, the strengthening effect of pearlite is weaker than that of martensite. However, SEM image (Fig. 10b) reveals small particles located within the ferrite grains. Considering the chemical composition of the microalloyed steel they could be carbides and/or carbonitrides of niobium and titanium. Their size and content are relatively large, which result from the high concentrations of Nb and Ti in this steel (Table 1). The identification of dispersive particles requires a more detailed analysis using TEM. The size of the phase α grains was restricted within the range of 4 to 13 µm.

3.5. Microstructure of the joints

The microstructure of the joints was typical of that made using laser welding. Fig. 11 presents the fusion zone of a characteristic dendritic form directed towards the joint centre. Fig. 12 shows the microstructure of the zone revealed at a greater magnification. During laser welding both the heating and cooling rates of steels were very high, leading to the formation of the martensitic structure in the weld material. Fig. 13 presents the microstructures of joints made at various welding rates, i.e. 5, 7, 8.5, and 9.5 m/min. All the fusion zones revealed the presence of lath martensite, with the laths being the greatest in the first case (Fig. 13a). An increase in a scanning rate was accompanied by a decrease in the lath sizes (Fig. 13b-d). This was due to an increase in the rate of heat discharge from the liquid metal pool. However, the cooling rate was not identical in all directions. When linear energy was insufficient to obtain the entire penetration, the heat discharge was faster from the bottom part of the weld than from the sides (due to the sheet thickness measured perpendicularly to the fusion line) (Fig. 14).

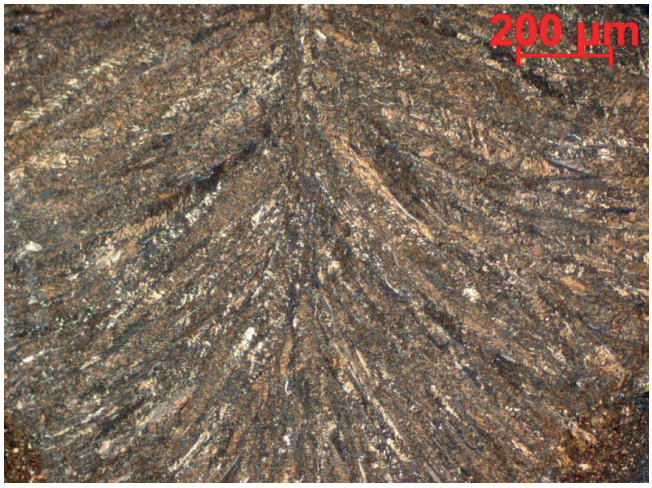

Fig. 11. Microstructure of the fusion zone magnified 100x

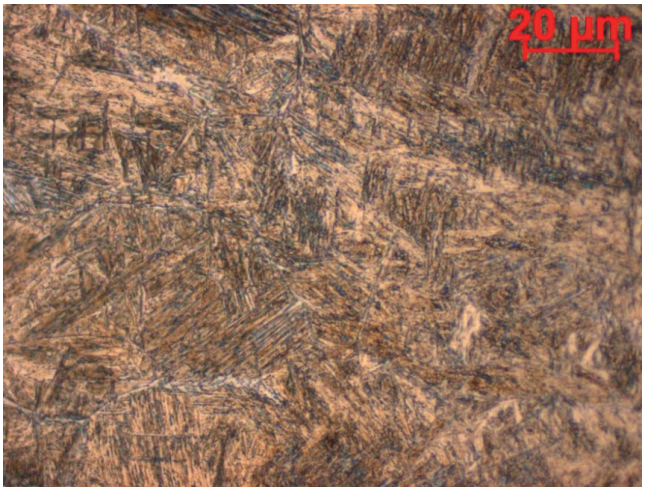

Fig. 12. Microstructure of the fusion zone magnified 1000x

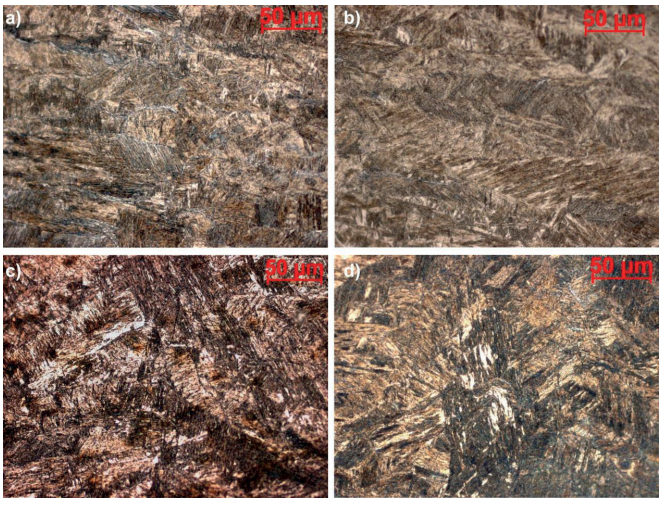

Fig. 13. Microstructure of the fusion zone of joints made at various

welding rates: a) V = 5 m/min, angle 90°, distance between the beams 0.6 mm; b) V = 7 m/min, angle 90°, distance between the beams 0.6 mm; c) V = 8.5m/min, angle 0°, distance between the beams: 1 mm; d) V = 9.5 m/min, angle 0°, distance between the beams 1 mm

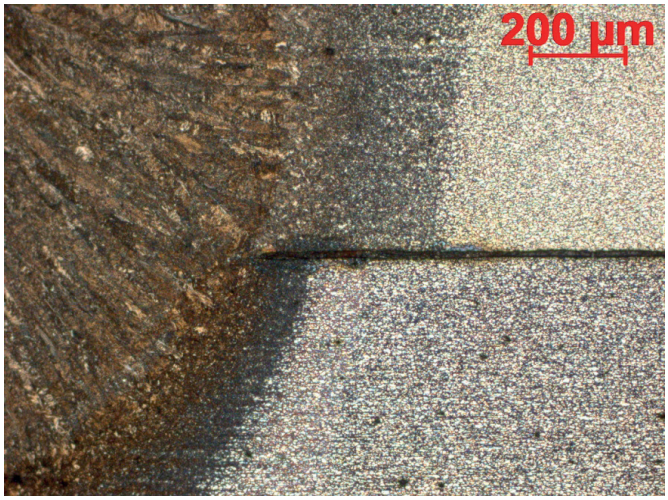

Fig. 14. Microstructure of a welded joint: the fusion zone, the HAZ and the base material; magnification: 100x

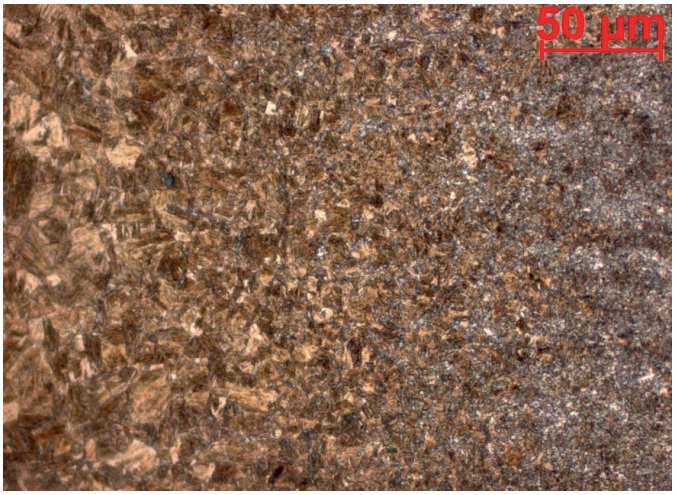

Fig. 15. Fragment of the HAZ in HSLA steel magnified 500x; V = 6 m/min, distance between the beams: 0.6 mm, angle 90°

Both the width and the distribution of the individual microstructural constituents resulted directly from welding conditions (e.g. welding rate related to linear energy). After performing the test where the entire penetration was not obtained (Fig. 14), it was possible to observe the difference between the HAZ width and the rate of changes taking place in the microstructure of both sheets along with an increase in the distance from the centre of the weld. The upper sheet (HSLA) was melted through. Therefore, the HAZ was wide and transitions between its successive areas were gentle. As regards the lower sheet (DP), the transitions between the individual zones of the microstructure were more intense.

Amirthalingam et al. [25] reported that a detrimental zone of polygonal ferrite can be formed near the fusion line in high-Al- or high-Si-containing steels. They found that these elements can partition from the liquid weld to the solidified delta ferrite in the fusion line resulting in ferrite stabilisation. This zone was wider for gas tungsten arc welded samples (smaller cooling rate) but a 50 µm wide ferrite zone was also formed for laser welded samples. This soft zone does not form in the present steels (Fig. 14) because the total content of Al+Si is limited below app. 0.5 wt.% (Table 1).

In both sheets the structural transformations took place in a different manner. This was due to differences in chemical compositions, phases, morphology and the heat input. Fig. 15 presents the smooth transitions between the overheated structure (on the left – thick-lath martensite in the HSLA steel) and the structure which underwent normalisation (on the right – fine-lath martensite in the HSLA steel). In the centre it is possible to observe the transient structure, in which the content of the fine-lath martensite increases gradually along with a decreasing distance from the base material (otherwise for the thick-lath martensite).

Unlike in the HSLA steel, in the DP steel the transition between the purely martensitic microstructure of the weld and the base material can be observed on a relatively narrow area. The entire HAZ is approximately three times narrower than in the HSLA steel and is approximately 100 µm in width. Fig. 16 presents a fragment of the HAZ of the DP steel. On the left it is possible to notice martensite; the content of the martensite decreases along with an increasing distance from the weld centre (to the right) (with increasingly ferrite grains visible). Kong et al. [17] reported that for increased laser powers the temperature gradient in the HAZ and hence grain growth are limited in DP steels.

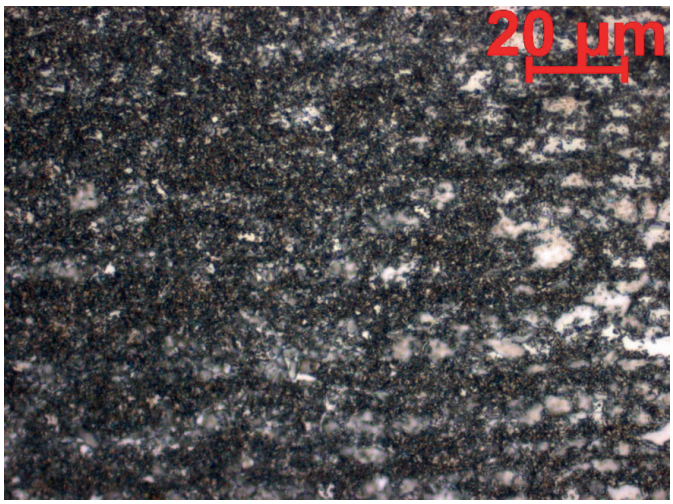

Fig. 16. Part of the HAZ in DP steel magnified 1000x; V = 6 m/min, distance between the beams 0.6 mm, angle 90°

Morphological details of the microstructure of the fusion and heat-affected zones can be revealed after applying scanning electron microscopy (SEM). The micrographs in Fig. 17a and b present a typical chaotic martensite microstructure of the fusion zone. The laths are oriented in different directions, which is characteristic for dendrite morphologies of fast cooled liquid pool. The martensite is a major structural constituent of the HAZ in both steels (Fig. 17c and d). There are no distinct differences between the microstructures of DP and HSLA steels. The HAZ is more fine-grained. There are no evidences of bainite, carbides or tempered martensite. It indicates that the second beam rather interferes with the first beam. It suggests that the distance between two spots should be larger than 1 mm to obtain tempering-like effects in the martensite.

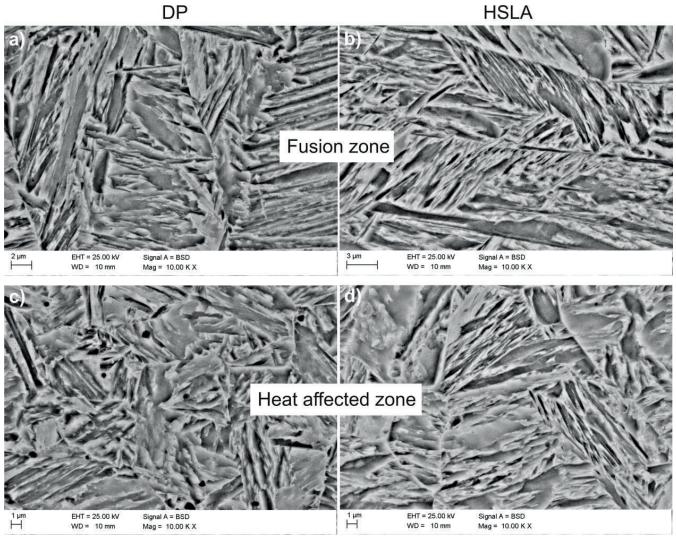

Fig. 17. SEM micrographs showing the microstructure of the fusion zone (a) and (b) and heat affected zone (c) and (d); V = 8.5 m/min, distance between the beams 1 mm, angle 0°

3.6. Hardness profiles

Hardness tests involved the joints without entire penetration – in order to obtain stricter results. Hardness was measured in the centre of the sheet thickness. The number of measurement spots amounted to 15. Fig. 18 presents the comparison of the average DP steel hardness with that of the HSLA steel on the cross-section of the joint. In the fusion zone the hardness values of the DP and HSLA steels were similar (between 420 and 430 HV5 for the DP steel area and between 410 and 420 HV5 for the HSLA steel area). These values are slightly higher compared to the maximum hardness obtained for the DP600 steel with a smaller strength level. Reisgen et al. [26] measured approximately 380 HV in the fusion zone. On the other hand the hardeness of the DP980 steel (with a higher strength level than the investigated DP800 steel) reaches 430-450 HV [27].

The values measured on both sides of the fusion zone of the investigated steels – in the HAZ – differed by 2-15 HV5 in the DP steel and by 0-17 HV5 in the HSLA steel. The hardness profile of the DP steel revealed a characteristic decrease in hardness (from 10 to 30 HV5) between the HAZ and the BM. This was due to the tempering of the martensite present in the DP steel. This softening was also observed by Sharma and Molian [28] in the DP980 steel. Farabi et al. [19] reported that the hardness softening increases along with an increase in the DP steel strength level. The average hardness of the DP steel base material amounted to 275 HV5, whereas in the HSLA to 205 HV5. The maximum hardness of both steels in the fusion zone amounted to approximately 420 HV5.

The use of two beams and their positions in relation to each other proved to affect the hardness and the width of joints (Fig. 19). As regards the HSLA steel, the difference in hardness in the fusion zone amounted to approximately 15 HV5, regardless of beam positioning. When a single beam was used, the fusion zone was the narrowest and characterised by the greatest hardness. The use of a dual beam in series widened the fusion zone and favourably decreased its hardness by approximately 20 HV5. Positioning the beams at an angle of 90° caused further widening of the fusion zone and decreased hardness to approximately 375 HV5 (i.e. by approximately 11%). As regards the welding of the DP steel, the scatter of hardness in the fusion zone for individual beam positions was up to 10 HV5 (Fig. 20). In this case, the hardness reduction in the fusion zone was not as significant as that observed for the HSLA steel, yet hardness decreased from 420 HV5 to 410 HV5 and 405 HV5 for the beams positioned at 0° and 90°, respectively. The hardness reduction in the soft zone did not significantly depend on beam positions.

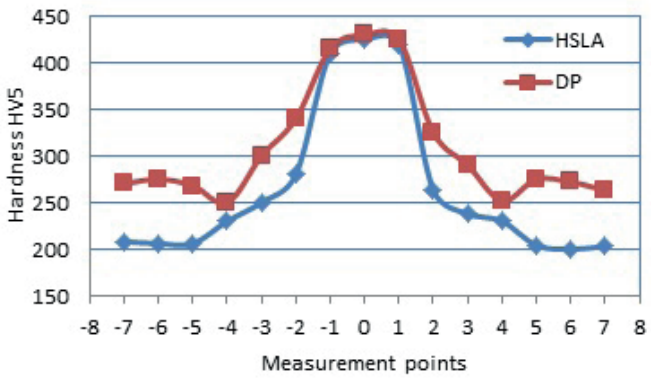

Fig. 18. Hardness distribution on the cross-section of the joint made with the single beam at a welding rate 11 m/min with the entire penetration

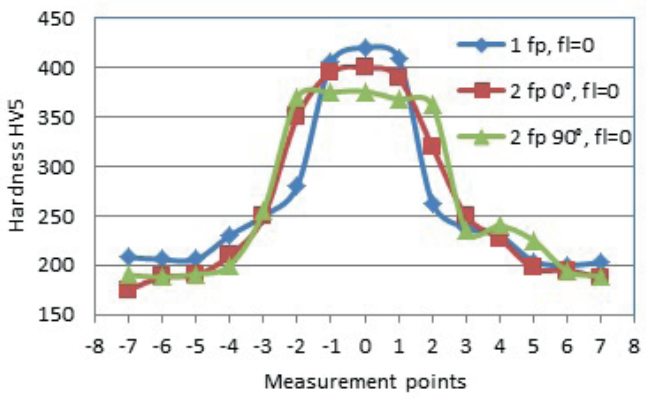

Fig. 19. Joint hardness distribution measured at the half of the HSLA steel sheet thickness for individual positions of laser beam focuses

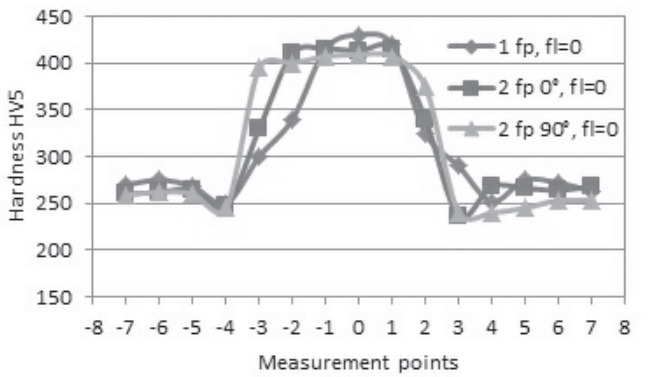

Fig. 20. Joint hardness distribution measured at the half of the DP steel sheet thickness for individual positions of laser beam focuses

4. Conclusions

The use of split laser beam changes the process of laser welding if compared with the process utilising a single beam. Distances between two laser beam focuses, positions of beams and welding rates affect the shape of penetration, the width of individual microstructural zones and the hardness of welded joints. In particular, it was drawn that:

- the greatest impact on the shape of welds and on obtained welding rates can be ascribed to the position of two focuses in relation to each other. Setting the focuses in series resulted in a slight reduction of welding rate ensuring the entire penetration of sheets. Positioning the focuses at 90° in relation to the direction of welding significantly reduced welding rate (to approximately 50% of the welding rate obtained during laser welding with the beam focused on one spot).
- the use of a beam split into two focuses favourably reduces hardness in the fusion zone to approximately 10% in comparison with hardness present in joints welded using classical techniques. The lower the welding rate (dependent on the positions of two focuses in relation to the direction of welding), the lower the hardness measured in the weld (375-420 HV5). Changes of beam positions have a greater effect on hardness reduction in HSLA than in DP steels.
- welding rates determine the shape and dimensions of the weld. The greater the scanning rate, the smaller the penetration of the lower sheet; the weld is similar to the letter V. A decrease in the rate is accompanied by an increase in the width of the joint of the sheets. Within the scanning rate of 5 to 12 m/min the microstructure of the fusion zone is composed of martensite, with lath sizes decreasing along with increasing welding rates.
- changes in inter-beam distances in the range of 0.6 mm to 1 mm do not significantly affect the geometrical dimensions of the joint, welding rates and the microstructure of the individual zones.

Acknowledgment

This publication was partially financed by the Ministry of Science and Higher Education of Poland as the statutory financial grant of the Faculty of Mechanical Engineering SUT.

REFERENCES

[1] S. Aslanlar, Mater. Design 27, 125-131 (2006).
[2] S. Stano, Weld. Int. 21, 809-813 (2007).
[3] J. Górka, Influence of welding thermal cycling on the join properties of S 700MC steel treated using thermomechanical method, in: J.F. Silva Gomez, M.A.P. Vaz (Eds.), Proc. of 15th Int. Conf. on Experimental Mechanics, Porto, Portugal, UNSP 2980 (2012).
[4] L. Konieczny, R. Burdzik, Solid State Phenom. 210, 26-31 (2014).
[5] J. Górka, Indian J. Eng. Mater. S. 22, (5), 497-502 (2015).
[6] A. Lisiecki, Metals 5, (1), 54-69 (2015).
[7] A. Grajcar, K. Radwanski, H. Krzton, Solid State Phenom. 203-204, 34-37 (2013).
[8] S. Lasek, E. Mazancova, Metalurgija, 52, 441-444 (2013).
[9] A. Grajcar, R. Kuziak, Adv. Mater. Res. 314-316, 119-122 (2011).
[10] M.S. Weglowski, K. Kwieciński, K. Krasnowski, R. Jachym, Arch. Civ. Mech. Eng. 9, (4), 85-97 (2009).
[11] M. Amirthalingam, M.J.M. Hermans, I.M. Richardson, Metall. Mater. Trans. A 40, 901-909 (2009).
[12] E. Skołek, K. Wasiak, W.A. Świątnicki, Mater. Tehnol. 49, (6), 933-939 (2015).
[13] A. Grajcar, M. Rożański, S. Stano, A. Kowalski, J. Mater. Eng. Perform. 23, 3400-3406 (2014).
[14] A. Lisiecki, Diode laser welding of high yield steel, in: W.L. Wolinski, Z. Jankiewicz, R.S. Romaniuk (Eds.), Proc. of SPIE, Laser Technology 2012: Application of Lasers, Szczecin, Poland, 8703, doi: 10.1117/12.2013429 (2013).
[15] M. Harooni, B. Carlson, R. Kovacevic, Opt. Laser Technol. 56, 247-255 (2014).
[16] S. Iqbal, M.M.S. Gualini, A. ur Rehman, Opt. Laser Technol. 42, 93-98 (2010).
[17] F. Kong, S. Santhanakrishnan, D. Lin, R. Kovacevic, J. Mater. Process. Tech. 209, 5996-6003 (2009).
[18] F. Nikoosohbat, S. Kheirandish, M. Goodarzi, M. Pouranvari, Mater. Tehnol. 49, 133-138 (2015).
[19] N. Farabi, D.L. Chen, J. Li, Y. Zhou, S.J. Dong, Mater. Sci. Eng. A 527, 1215-1222 (2010).
[20] X. Li, L. Wang, L. Yang, J. Wang, K. Li, J. Mater. Process. Tech. 214, 1844-1851 (2014).
[21] L. Cretteur, A.I. Koruk, L. Tosal-Martinez, Steel Res. 73, 314-319 (2002).
[22] J. Xie, Welding J. 10, 223-230 (2002).
[23] T. Nilsson, Welding of AHSS/UHSS Steel – A Guide for the Automotive Industry, SSAB, Osterbergs 2012.
[24] A. Grajcar, M. Rożański, S. Stano, A. Kowalski, B. Grzegorczyk, Adv. Mater. Sci. Eng. 2014, 8 pages, doi. org/10.1155/2014/658947 (2014).
[25] M. Amirthalingam, M.J.M. Hermans, I.M. Richardson, Adv. Mater. Res. 89-91, 23-28 (2010).
[26] U. Reisgen, M. Schleser, O. Mokrov, E. Ahmed, J. Mater. Process. Tech. 210, 2188-2196 (2010).
[27] J. Ma, F. Kong, B. Carlson, R. Kovacevic, J. Mater. Process. Tech. 213, 495-507 (2013).
[28] R.S. Sharma, P. Molian, J. Mater. Process. Tech. 211, 1888-1897 (2011).